AIMS Mathematics, 10(2): 4092–4119.
DOI: 10.3934/math.2025190
Received: 10 December 2024
Revised: 13 February 2025
Accepted: 20 February 2025
Published: 27 February 2025

https://www.aimspress.com/journal/Math

Research article

Qualitative analysis and new traveling wave solutions for the stochastic Biswas-Milovic equation

Dan Chen[1,2,*], **Da Shi**[1] **and Feng Chen**[3]

[1] College of Computer Science, Chengdu University, Chengdu 610106, China
[2] Visual Computing and Virtual Reality Key Laboratory of Sichuan Province, Sichuan Normal University, Chengdu 610068, China
[3] School of Mechanical Engineering, Chengdu University, Chengdu 610106, China

* **Correspondence:** Email: chendan@cdu.edu.cn.

Abstract: In this paper, we investigated the planar dynamical system and new traveling wave solution of the stochastic Biswas-Milovic equation (BME) with dual-power law nonlinearity and multiplicative white noise in the Itô sense. First, the stochastic BME with dual-power law nonlinearity and multiplicative white noise in the Itô sense was transformed into a nonlinear ordinary differential equation (NLODE) through traveling wave transformation. Second, the dynamical bifurcation conditions and phase diagrams of the equation considered were obtained through the method of planar dynamical systems, and the phase portrait of the dynamical system was given. Moreover, taking into account the periodic disturbances in real-world environments, we extended our analysis to explore the effects of disturbance terms. Meanwhile, two-dimensional (2D) and three-dimensional (3D) phase portraits, sensitivity analyses, and the Poincaré section of its perturbed system were plotted through Maple software. Finally, the new traveling wave solutions of the stochastic BME with dual-power law nonlinearity and multiplicative white noise in the Itô sense were constructed by using the complete discrimination system method.

Keywords: stochastic Biswas-Milovic equation; planar dynamical system; traveling wave solutions; complete discrimination system
Mathematics Subject Classification: 35B20, 35B32, 35C07, 60H15

1. Introduction

The study of the exact solutions and dynamical behavior of nonlinear equations not only helps to understand the essential properties and algebraic structure of soliton theory [1–3], but also plays an important role in the rational explanation and practical application of corresponding natural

phenomena [4–6]. For instance, the Biswas-Milovic equation (BME) has attracted widespread attention for its ability to describe nonlinear wave dynamics and mode formation in various physical systems [7–9]. Meanwhile, the stochastic BME is an extended form that incorporates the effects of random perturbations or noise, providing a more accurate reflection of dynamic behaviors in complex environments in practical applications [10, 11]. In the field of optics and photonics, the stochastic BME can be used to describe the propagation behavior of optical pulses in fiber communication systems [12], especially in the presence of random noise such as thermal noise or phase noise. Within fluid mechanics, this equation can also be employed to simulate the nonlinear evolution of water surface waves [13–15], particularly when the waves are influenced by random factors such as stochastic wind fields or other external random effects.

The addition of multiplicative white noise further enriches the descriptive power of the equation. Unlike additive noise, which assumes that external random fluctuations uniformly affect the system, multiplicative noise implies that the strength of randomness depends on the state of the system itself. This feature is particularly relevant when fluctuations are inherently related to the size of the variables they affect, thus capturing important aspects of real-world complexity and uncertainty.

In recent years, numerous experts in physics and mathematics have investigated the solutions of the BME employing a variety of classic and intriguing methods [16–18]. However, there remains limited analysis concerning the bifurcation and chaotic behavior of the BME [19–21]. Our research work is significant because we have not only enriched the solutions of the BME applying the polynomial complete discriminant system method, but also conducted a thorough analysis of the planar dynamical system applying the planar dynamical system method. The findings we have obtained provide insight into the chaotic nature of the framework under examination, thereby enhancing our understanding of the dynamics that underlie it. While our methods demonstrate systematicness, precision, broad applicability, and deep theoretical underpinnings, they do possess certain limitations, particularly when addressing high-dimensional problems, which often necessitate the integration of other approaches, such as numerical simulation methods. Notwithstanding this limitation, current research suggests that the methods employed in this work are highly reliable, versatile, and effective for a variety of nonlinear models across different scientific disciplines.

The stochastic BME with dual-power law nonlinearity and multiplicative white noise in the Itô sense was introduced by Elsayed et al. in [22]. It can be expressed as follows:

$$i(q^m)_t + a(q^m)_{xx} + (b|q|^{2n} + c|q|^{4n})q^m + m\sigma q^m \frac{\partial W(t)}{\partial t} = 0, \tag{1.1}$$

where $i^2 = -1$,

$$q = q(x, t)$$

is a complex-valued function related to wave profile, and the independent variables x and t denote the distance and time, respectively. Meanwhile, m is the maximum intensity parameter, and a, b and c are real-values constants, where a represents generalized chromatic dispersion, while b and c represent double-power nonlinearity. Besides, n is the parameter of the power law nonlinearity, $W(t)$ is the standard Wiener process, and $\frac{\partial W(t)}{\partial t}$ is the formal derivative of the Wiener process with respect to time, which represents multiplicative white noise used to identify the process where the excitation phase is interrupted. Notably, σ is a positive constant denoting the noise strength coefficient, and the well-known BME with dual-power law nonlinearity is the case where $\sigma = 0$ in Eq (1.1).

The interaction between double power nonlinearity and multiplicative white noise poses serious challenges for analysis and numerical research. The purpose of this article is to study the planar dynamical system and new traveling wave solution of Eq (1.1) in order to reveal the complex network of stability, bifurcation, and pattern formation under random influence, and to elucidate the mechanisms driving unpredictable behavior in natural and engineering systems. To the best our knowledge, no literature has used this method before. Therefore, the research findings of this article contribute to make a comprehensive and systemic study on the propagation dynamics of Eq (1.1) with different methods.

This article consists of the several parts as follows: In Section 2, Eq (1.1) is first transformed into a nonlinear ordinary differential equation (NLODE) with taking traveling wave transformation, and then a second-order NLODE is obtained by applying the trial method of polynomial for rank homogeneous equations and the homogeneous equilibrium principle of polynomials. In Section 3, the dynamical bifurcation conditions and phase diagrams of the equation considered are obtained through the method of planar dynamical systems. Moreover, the phase portrait of the dynamical system is given. Meanwhile, two-dimensional (2D) and three-dimensional (3D) phase portrait, sensitivity analyses and Poincaré section of its perturbation system are plotted by Maple. In Section 4, the optical soliton solutions of the BME with dual-power law nonlinearity and multiplicative white noise in the Itô sense are constructed by using the complete discrimination system method. Finally, a brief conclusion is given in Section 5.

2. Mathematical analysis

To solve Eq (1.1), we consider the solution in the following form:

$$q(x,t) = Q(\xi)\exp i[\eta(x,t) + \sigma W(t) - \sigma^2 t], \quad \eta(x,t) = -\kappa x + \omega t, \quad \xi = x - Vt, \tag{2.1}$$

where κ, ω, V are nonzero real values, while $Q(\xi)$ and $\eta(x,t)$ are real-valued functions. More precisely, $Q(\xi)$ and $\eta(x,t)$ represent the amplitude and phase components of the soliton, respectively. In Eq (2.1), ξ is the wave variable, ω is the wave number, κ is the frequency, and V is the velocity of the soliton.

Substituting (2.1) into (1.1), and setting the real and imaginary parts separately equal to zero, we can obtain

$$amQQ'' + am(m-1)Q'^2 - m(\omega - \sigma^2 + am\kappa^2)Q^2 + bQ^{2n+2} + cQ^{4n+2} = 0 \tag{2.2}$$

and

$$m(V + 2am\kappa)Q' = 0. \tag{2.3}$$

From (2.3), we derive the velocity

$$V = -2am\kappa.$$

Remark 2.1. *Due to κ, V being nonzero real values and satisfying*

$$V = -2am\kappa,$$

the case when $a < 0$, $m > 0$, and $\kappa > 0$ is our main focus in the following part.

Next, setting

$$Q = H^{\frac{1}{2n}}, \quad n \geq 1,$$

we can reduce (2.2) to the following form of integer balance number:

$$am[2nHH^{''} + (m-2n)H^{'2}] - 4n^2m(\omega - \sigma^2 + am\kappa^2)H^2 + 4n^2bH^3 + 4n^2cH^4 = 0. \tag{2.4}$$

Then, with the trial method [23–25] of polynomial for rank homogeneous equations and the principle of homogeneous balance, we can get the trial equation as follows:

$$H^{''} = \alpha_0 + \alpha_1 H + \alpha_2 H^2 + \alpha_3 H^3, \tag{2.5}$$

where $\alpha_j (j = 1, 2, 3)$ are all constants. After that, multiplying both sides of (2.5) by $H^{'}$, integrating once, and converting the coefficient of $(H^{'})^2$ to integer, we yield

$$(H^{'})^2 = 2\alpha_0 H + \alpha_1 H^2 + \frac{2\alpha_2}{3}H^3 + \frac{\alpha_3}{2}H^4 + d_0, \tag{2.6}$$

where d_0 is an integral constant.

Substituting (2.5) and (2.6) into (2.4), an algebraic equation about H is obtained. By setting the coefficients to zero, we arrive at

$$\alpha_0 = 0, \quad \alpha_1 = \frac{4n^2(\omega - \sigma^2 + am\kappa^2)}{am}, \quad \alpha_2 = -\frac{6n^2b}{am(m+n)}, \quad \alpha_3 = -\frac{8n^2c}{am(m+2n)}, \quad d_0 = 0$$

in the case of $m \neq n$.

Remark 2.2. *If $m = n$, apart from $\alpha_0 \in R$ differing from the results obtained previously, the values of the other parameters α_1–α_3, and d_0 are calculated by substituting $m = n$ into the corresponding coefficient expressions that were established in the case of $m \neq n$, that is,*

$$\alpha_0 \in R, \quad \alpha_1 = \frac{4n(\omega - \sigma^2 + an\kappa^2)}{a}, \quad \alpha_2 = -\frac{3b}{a}, \quad \alpha_3 = -\frac{8c}{3a}, \quad d_0 = 0.$$

Remark 2.3. *If*

$$m = 2n,$$

which reduces (2.4) to

$$H^{''} = \frac{2n}{a}(\omega - \sigma^2 + 2an\kappa^2)H - \frac{b}{a}H^2 - \frac{c}{a}H^3,$$

that is, the result calculated by substituting $m = 2n$ into the corresponding coefficient expressions in the case of $m \neq n$.

3. Qualitative analysis of Eq (2.5)

In this section, we consider the dynamical behavior of Eq (2.5) in the case of $m \neq n$. When $m \neq n$, the Eq (2.5) becomes

$$H^{''} = \alpha_1 H + \alpha_2 H^2 + \alpha_3 H^3. \tag{3.1}$$

First, we set

$$\frac{dH}{d\xi} = U.$$

Second, we convert Eq (3.1) into the two-dimensional Hamiltonian system

$$\begin{cases} \frac{dH}{d\xi} = U, \\ \frac{dU}{d\xi} = \alpha_1 H + \alpha_2 H^2 + \alpha_3 H^3. \end{cases} \tag{3.2}$$

The Hamiltonian function is

$$\Gamma(H, U) = \frac{1}{2}U^2 - \frac{\alpha_3}{4}H^4 - \frac{\alpha_2}{3}H^3 - \frac{\alpha_1}{2}H^2 = \frac{d_0}{2}. \tag{3.3}$$

Here, $d_0 = 0$, i.e., the value of d_0 is fixed and unchanged, which means that (3.3) determines the family of invariant curves for system (3.2).

Third, we consider the phase diagram branches of Hamiltonian system (3.2). Supposing that

$$G(H) = (\alpha_3 H^2 + \alpha_2 H + \alpha_1)H,$$

and assuming that the matrix

$$M(H_i, 0) = \begin{pmatrix} 0 & 1 \\ 3\alpha_3 H_i^2 + 2\alpha_2 H_i + \alpha_1 & 0 \end{pmatrix},$$

where H_i ($i \in \{0, 1, 2, 3, \cdots\}$) is the real root of

$$G(H_i) = 0.$$

It is obvious that

$$\det(M(H_i, 0)) = -(3\alpha_3 H_i^2 + 2\alpha_2 H_i + \alpha_1).$$

Further, set

$$\Delta = \alpha_2^2 - 4\alpha_1\alpha_3.$$

Then, on the basis of the theory of planar dynamical systems, we classify the trajectories near the equilibrium point and draw the corresponding phase diagram using the Maple software, which are listed in Figures 1–3. Here, symbols $(+, -, +)$ in these figures denote $\alpha_1 > 0$, $\alpha_2 < 0$, and $\alpha_3 > 0$, while, $(+, 0, +)$ in these figures denote $\alpha_1 > 0$, $\alpha_2 = 0$, and $\alpha_3 > 0$. The conclusion is

Proposition 3.1. *Assume that* $\mathbf{E}_i(H_i, 0)$ *is the equilibrium point of Eq (3.2).*

Case I. $\Delta < 0$.

When $\alpha_1 > 0$, *we obtain* $\det(M(0, 0)) < 0$, *then* $\mathbf{E}_0(0, 0)$ *is the saddle point. In addition, the colors of the branch trajectories are the same, and it indicates that the system (3.2) has a doubly-periodic function solution (see Figure 1a,b).*

When $\alpha_1 < 0$, *we obtain* $\det(M(0, 0)) > 0$, *then* $\mathbf{E}_0(0, 0)$ *is the center point. In addition, the closed curve appears, which indicates the path of the system in phase space during periodic repetitive motion and the system (3.2) has a family of periodic solutions (see Figure 1c,d).*

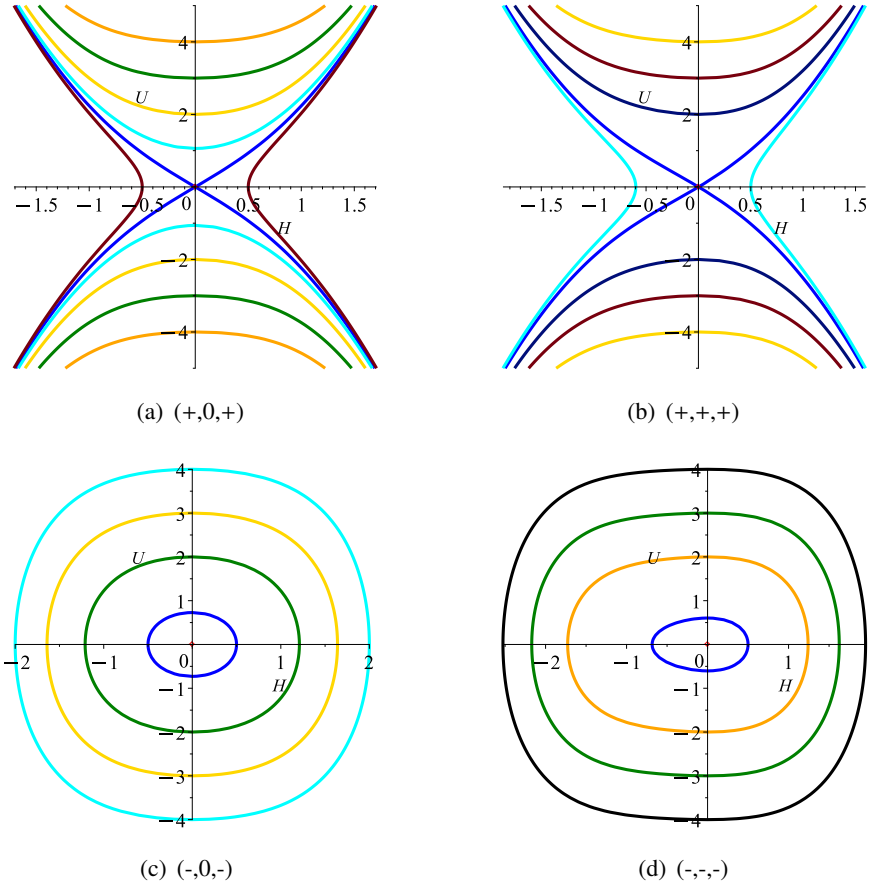

(a) (+,0,+) (b) (+,+,+)

(c) (-,0,-) (d) (-,-,-)

Figure 1. The phase portraits of (3.2) for $\Delta < 0$.

Case II. $\Delta > 0$.

When $\alpha_1 > 0$, *we obtain* $\det(M(0,0)) < 0$, *then* $\mathbf{E}_0(0,0)$ *is the saddle point.*

When $\alpha_1 < 0$, *we obtain* $\det(M(0,0)) > 0$, *then* $\mathbf{E}_0(0,0)$ *is the center point.*

When $\alpha_2 < 0$, $\alpha_3 > 0$, *or* $\alpha_1 < 0$, $\alpha_2 > 0$, $\alpha_3 > 0$, *or* $\alpha_1 < 0$, $\alpha_2 > 0$, $\alpha_3 < 0$, *and we obtain*

$$\det(M(\frac{-\alpha_2 + \sqrt{\Delta}}{2\alpha_3}, 0)) < 0,$$

then $\mathbf{E}_1(\frac{-\alpha_2+\sqrt{\Delta}}{2\alpha_3}, 0)$ *is the saddle point.*

When $\alpha_2 > 0$, $\alpha_3 < 0$, *or* $\alpha_1 > 0$, $\alpha_2 > 0$, $\alpha_3 < 0$, *or* $\alpha_1 > 0$, $\alpha_2 > 0$, $\alpha_3 > 0$, *and we obtain*

$$\det(M(\frac{-\alpha_2 + \sqrt{\Delta}}{2\alpha_3}, 0)) > 0,$$

then $\mathbf{E}_1(\frac{-\alpha_2+\sqrt{\Delta}}{2\alpha_3}, 0)$ *is the center point.*

When $\alpha_2 > 0$, $\alpha_3 > 0$, *or* $\alpha_1 < 0$, $\alpha_2 < 0$, $\alpha_3 < 0$, *or* $\alpha_1 < 0$, $\alpha_2 < 0$, $\alpha_3 > 0$, *and we obtain*

$$\det(M(\frac{-\alpha_2 - \sqrt{\Delta}}{2\alpha_3}, 0)) < 0,$$

then $\mathbf{E}_2(\frac{-\alpha_2-\sqrt{\Delta}}{2\alpha_3}, 0)$ *is the saddle point.*

When $\alpha_2 > 0$, $\alpha_3 < 0$, *or* $\alpha_1 > 0$, $\alpha_2 < 0$, $\alpha_3 > 0$, *or* $\alpha_1 > 0$, $\alpha_2 < 0$, $\alpha_3 < 0$, *and we obtain*

$$\det(M(\frac{-\alpha_2 - \sqrt{\Delta}}{2\alpha_3}, 0)) > 0,$$

then $\mathbf{E}_2(\frac{-\alpha_2-\sqrt{\Delta}}{2\alpha_3}, 0)$ *is the center point.*

In addition, Figure 2b,c indicates that the system (3.2) has a kink wave, while Figure 2a,d indicates that the system (3.2) has the homoclinic orbits, the periodic orbits, and the bounded open orbits.

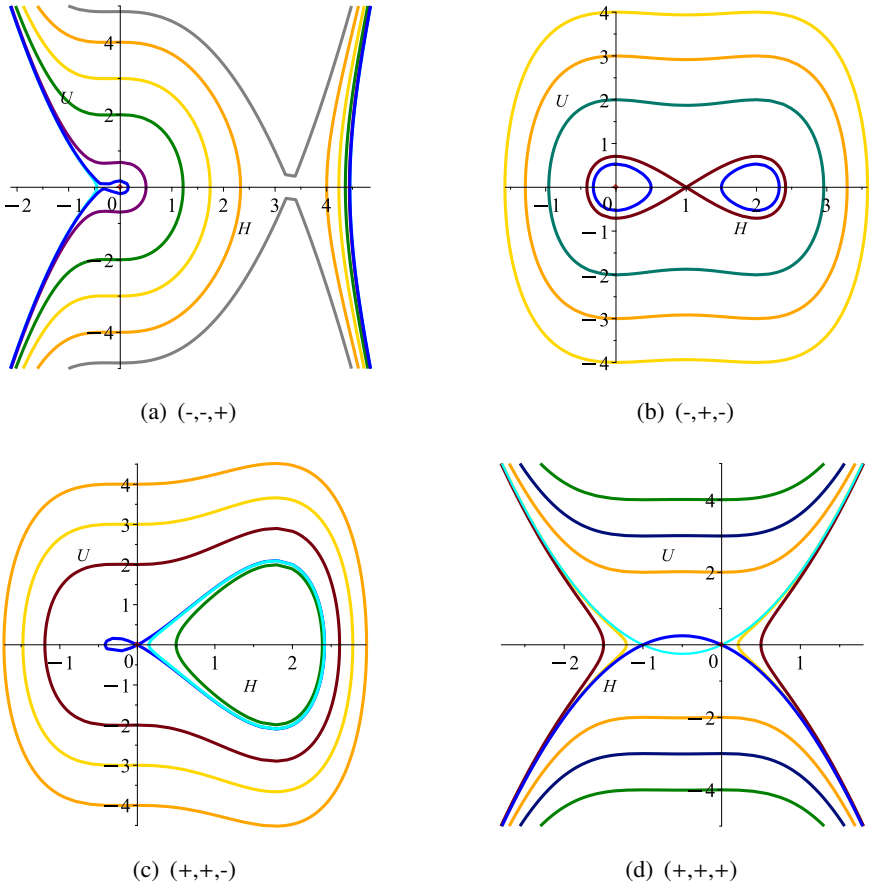

(a) (-,-,+) (b) (-,+,-)

(c) (+,+,-) (d) (+,+,+)

Figure 2. The phase portraits of (3.2) for $\Delta > 0$.

Case III. $\Delta = 0$.

When $\alpha_1 > 0$, *we obtain* $\det(M(0,0)) < 0$, *then* $\mathbf{E}_0(0,0)$ *is the saddle point.*

When $\alpha_1 < 0$, *we obtain* $\det(M(0,0)) > 0$, *then* $\mathbf{E}_0(0,0)$ *is the center point.*

When

$$\det(M(-\frac{\alpha_2}{2\alpha_3}, 0)) = 0,$$

and the Poincaré index of it is equal to zero, then $\mathbf{E}_3(-\frac{\alpha_2}{2\alpha_3}, 0)$ *is the cusp point. For instance,* $\mathbf{E}_3(1,0)$ *in Figure 3a,* $\mathbf{E}_3(-2,0)$ *in Figure 3b, and* $\mathbf{E}_3(-1,0)$ *in Figure 3c.*

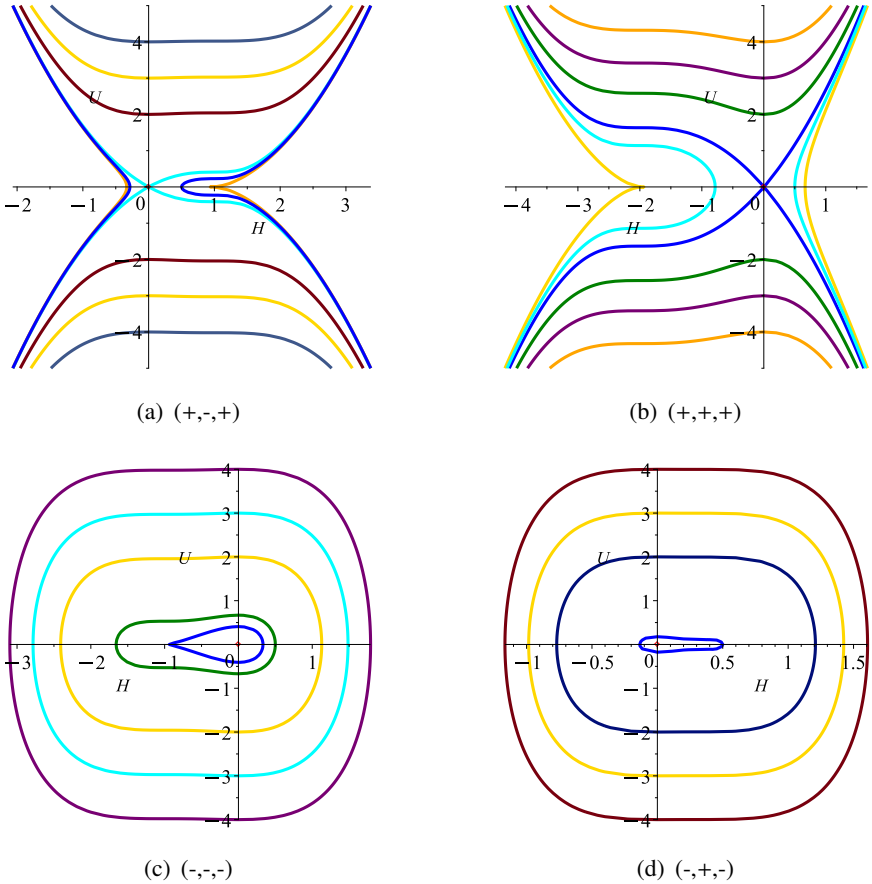

(a) (+,-,+) (b) (+,+,+)

(c) (-,-,-) (d) (-,+,-)

Figure 3. The phase portraits of (3.2) for $\Delta = 0$.

Considering that periodic interference often exists in real environments, here we add periodic perturbations and small perturbations to system (3.2), respectively,

$$\begin{cases} \frac{dH}{d\xi} = U, \\ \frac{dU}{d\xi} = \alpha_1 H + \alpha_2 H^2 + \alpha_3 H^3 + \Upsilon(\xi), \end{cases} \tag{3.4}$$

where

$$\Upsilon(\xi) = A\sin(\iota\xi)$$

or

$$\Upsilon(\xi) = Ae^{\iota\xi}$$

is the perturbed term, with A and ι being two real constants. In Figures 4–7, we consider the sensitivity of Eq (3.4) in different initial values and the impact of A, ι on the solution behavior. Setting

$$a = -1, \quad b = 3, \quad c = -1, \quad n = 1, \quad \omega = 4, \quad \kappa = 1$$

unchanged, the values of α_1–α_3 change with the vary value of m and σ. Here, $m = 2, \sigma = 1$ correspond to

$$\alpha_1 = -2, \quad \alpha_2 = 3, \quad \alpha_3 = -1,$$

while, $m = 5, \sigma = 2$ correspond to

$$\alpha_1 = 4, \quad \alpha_2 = 0.6, \quad \alpha_3 = -\frac{8}{35}.$$

Under the condition of changes in parameters, we use 2D trajectories (see Figures 4a–7a), 3D trajectories(see Figures 4b–7b), sensitivity analyses (see Figures 4c–7c), and Poincaécross-sections (see Figures 4d–7d) to demonstrate the impact of perturbations on solution behavior sepatately. As shown in the grahs, chaos behavior, periodic behavior, and quasi periodic behavior are present by adding perturbation terms. The variation in noise intensity may lead to the transformation of the system's chaotic behavior into periodic motion, while minor variations in the intensity and frequency of external interference may have little impact on the system.

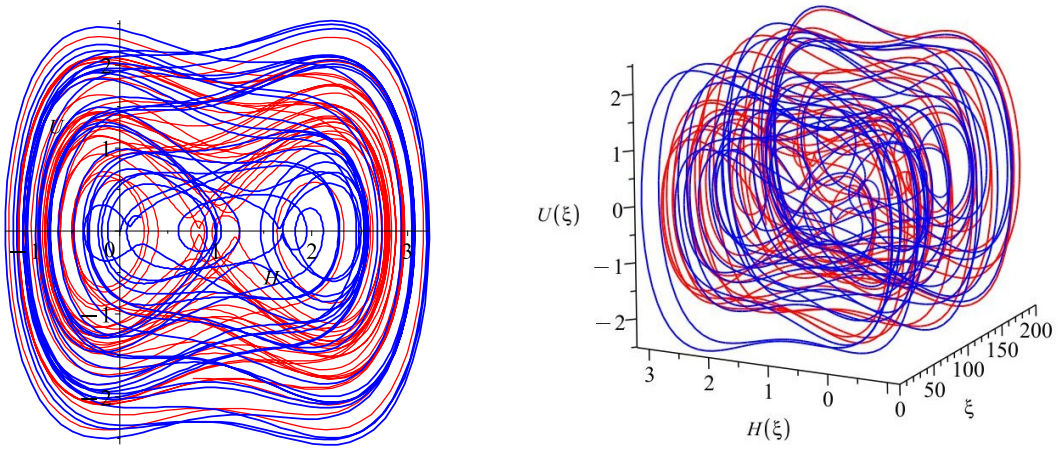

(a) 2D trajectories

(b) 3D trajectories

(c) Sensitivity analyses

(d) Poincaécross-sections

Figure 4. Chaotic behavior of Eq (3.4) for $\alpha_1 = -2$, $\alpha_2 = 3$, $\alpha_3 = -1$, $m = 2$, $\sigma = 1$, $A = 0.6$ and $\iota = 0.8$, where $\Upsilon(\xi) = A\sin(\iota\xi)$.

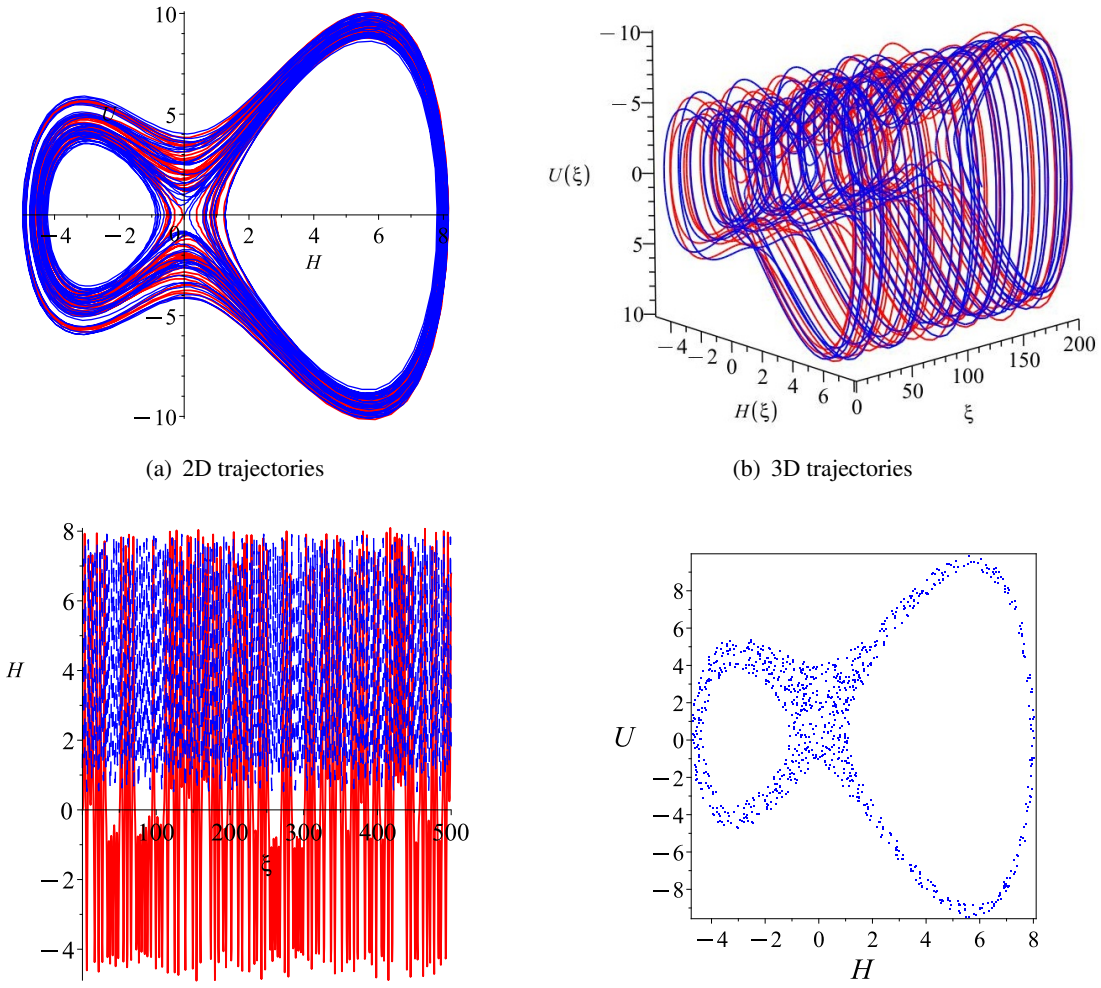

(a) 2D trajectories

(b) 3D trajectories

(c) Sensitivity analyses

(d) Poincaécross-sections

Figure 5. Chaotic behavior of Eq (3.4) for $\alpha_1 = 4$, $\alpha_2 = 0.6$, $\alpha_3 = -\frac{8}{35}$, $m = 5$, $\sigma = 2$, $A = 0.6$ and $\iota = 0.8$, where $\Upsilon(\xi) = A\sin(\iota\xi)$.

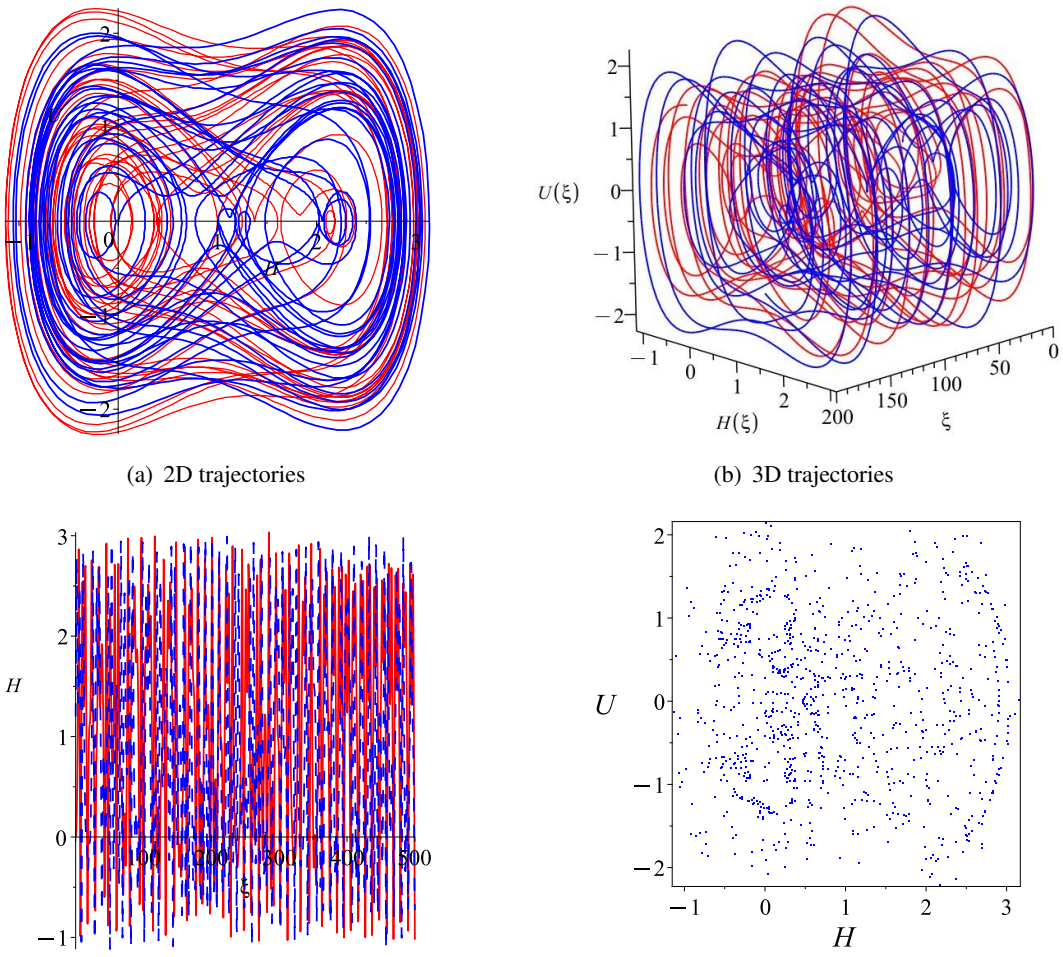

(a) 2D trajectories

(b) 3D trajectories

(c) Sensitivity analyses

(d) Poincaécross-sections

Figure 6. Chaotic behavior of Eq (3.4) for $\alpha_1 = -2$, $\alpha_2 = 3$, $\alpha_3 = -1$, $m = 2$, $\sigma = 1$, $A = 0.7$ and $\iota = 0.6$, where $\Upsilon(\xi) = A\sin(\iota\xi)$.

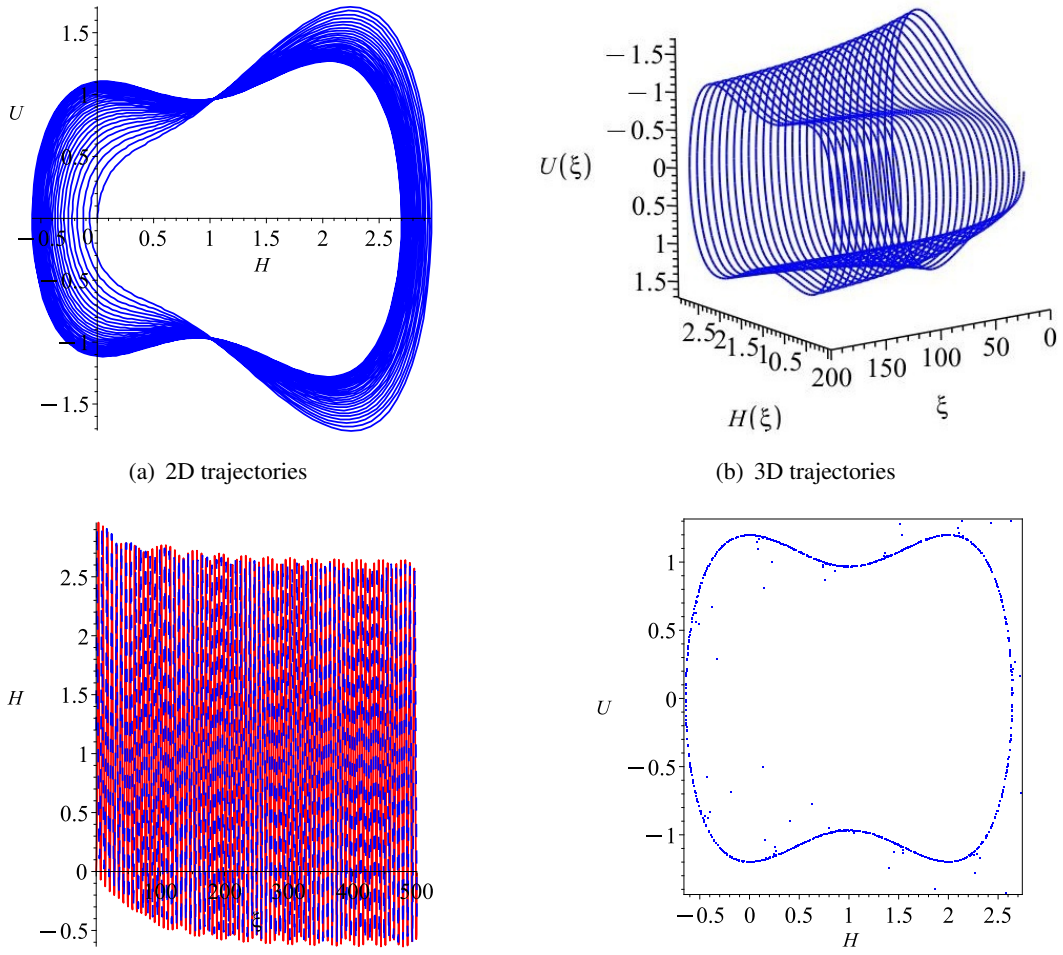

(a) 2D trajectories

(b) 3D trajectories

(c) Sensitivity analyses

(d) Poincaécross-sections

Figure 7. Chaotic behavior of Eq (3.4) for $\alpha_1 = -2$, $\alpha_2 = 3$, $\alpha_3 = -1$, $m = 2$, $\sigma = 1$, $A = 0.7$ and $\iota = -0.01$, where $\Upsilon(\xi) = Ae^{\iota\xi}$.

4. Traveling wave solutions of Eq (1.1)

In this section, we seek for the new traveling wave solutions of Eq (1.1) by applying the complete discriminant method.

4.1. The case of $m \neq n$

In this scenario, Eq (2.6) becomes

$$(H^{'})^2 = \alpha_1 H^2 + \frac{2\alpha_2}{3} H^3 + \frac{\alpha_3}{2} H^4. \tag{4.1}$$

With the condition of

$$(p_3 H^2 + p_2 H + p_1)H \neq 0,$$

by calculation, Eq (4.1) can be rewritten as following using elementary integration:

$$\pm(\xi - \xi_0) = \int \frac{dH}{H\sqrt{p_3H^2 + p_2H + p_1}}, \tag{4.2}$$

where

$$p_3 = \frac{1}{2}\alpha_3, \quad p_2 = \frac{2}{3}\alpha_2, \quad p_1 = \alpha_1,$$

ξ_0 is the integral constant.

Remark 4.1. *If*

$$(p_3H^2 + p_2H + p_1)H = 0,$$

the solution of Eq (1.1) is

$$q(x,t) = \varkappa^{\frac{1}{2n}} \exp i[-\kappa x + \omega t + \sigma W(t) - \sigma^2 t],$$

where $\varkappa$ is an arbitrary constant.

Setting

$$F(H) = p_3H^2 + p_2H + p_1.$$

In the rest part, with the complete discriminant system of the second order polynomial, by the root of $F(H)$, the traveling wave solution of Eq (1.1) has the following implicit solutions for three situations:

Case 1. When

$$b^2(m + 2n) + 4c(\omega - \sigma^2 + am\kappa^2)(m + n)^2 = 0,$$

namely,

$$F(H) = p_3(H + \frac{p_2}{2p_3})^2,$$

also if

$$\frac{8n^2c}{am(m + 2n)} < 0,$$

the traveling wave solution of Eq (4.1) is given as

$$\xi - \xi_0 = \pm\frac{2p_3^{\frac{1}{2}}}{p_2} \ln|\frac{H}{H + \frac{p_2}{2p_3}}|, \tag{4.3}$$

provided

$$H + \frac{p_2}{2p_3} \neq 0.$$

Remark 4.2. *If*

$$H + \frac{p_2}{2p_3} = 0,$$

that is,

$$H = -\frac{b(m + 2n)}{2c(m + n)},$$

then the solution of Eq (1.1) is

$$q(x,t) = [-\frac{b(m + 2n)}{2c(m + n)}]^{\frac{1}{2n}} \exp i[-\kappa x + \omega t + \sigma W(t) - \sigma^2 t].$$

Case 2. When

$$b^2(m+2n)+4c(\omega-\sigma^2+am\kappa^2)(m+n)^2>0,$$

namely,

$$F(H)=p_3(H+\frac{p_2}{2p_3})^2-\frac{p_2^2-4p_1p_3}{4p_3};$$

(I) If

$$\frac{8n^2c}{am(m+2n)}<0,$$

there are three forms of solutions to Eq (4.1) as below:

$$\pm\sqrt{p_3}(\xi-\xi_0)=\frac{1}{\sqrt{\varrho_1\varrho_2}}\ln\frac{[\sqrt{(-\varrho_2)(H-\varrho_1)}-\sqrt{(-\varrho_1)}(H-\varrho_2)]^2}{|H|},\tag{4.4}$$

$$\pm\sqrt{p_3}(\xi-\xi_0)=\frac{1}{\sqrt{\varrho_1\varrho_2}}\ln\frac{[\sqrt{\varrho_2(H-\varrho_1)}-\sqrt{\varrho_1(H-\varrho_2)}]^2}{|H|},\tag{4.5}$$

$$\pm\sqrt{p_3}(\xi-\xi_0)=\frac{1}{\sqrt{-\varrho_1\varrho_2}}\arcsin\frac{(-\varrho_2)(H-\varrho_1)+(-\varrho_1)(H-\varrho_2)}{|H||\varrho_1-\varrho_2|}.\tag{4.6}$$

(II) If

$$\frac{8n^2c}{am(m+2n)}>0,$$

there are another three forms of solutions to Eq (4.1) as below:

$$\pm\sqrt{-p_3}(\xi-\xi_0)=\frac{1}{\sqrt{-\varrho_1\varrho_2}}\ln\frac{[\sqrt{(-\varrho_2)(H+\varrho_1)}-\sqrt{\varrho_1}(H-\varrho_2)]^2}{|H|},\tag{4.7}$$

$$\pm\sqrt{-p_3}(\xi-\xi_0)=\frac{1}{\sqrt{-\varrho_1\varrho_2}}\ln\frac{[\sqrt{\varrho_2(-H+\varrho_1)}-\sqrt{(-\varrho_1)(H-\varrho_2)}]^2}{|H|},\tag{4.8}$$

$$\pm\sqrt{-p_3}(\xi-\xi_0)=\frac{1}{\sqrt{\varrho_1\varrho_2}}\arcsin\frac{[\sqrt{(-\varrho_2)(H+\varrho_1)}-\sqrt{\varrho_1}(H-\varrho_2)]^2}{|H|},\tag{4.9}$$

where assuming that the internal scores of the radical are all greater than zero in (4.4)–(4.9), and

$$\varrho_1=\frac{-p_2+\sqrt{p_2^2-4p_1p_3}}{2p_3},\quad \varrho_2=\frac{-p_2-\sqrt{p_2^2-4p_1p_3}}{2p_3}.$$

Case 3. When

$$b^2(m+2n)+4c(\omega-\sigma^2+am\kappa^2)(m+n)^2<0,$$

the equality

$$F(H)=0$$

has no real root; also if

$$\frac{4n^2(\omega-\sigma^2+am\kappa^2)}{am}>0,$$

the traveling wave solution of Eq (4.1) is given as

$$\pm\frac{1}{\sqrt{p_3}}(\xi-\xi_0)=\frac{1}{\sqrt{p_1}}\ln|\frac{\frac{p_2}{\sqrt{p_1}}H+\sqrt{p_1}-\sqrt{p_3H^2+p_2H+p_1}}{\sqrt{p_3}H}|, \tag{4.10}$$

provided $p_1, p_3 > 0$.

The new traveling wave solutions of Eq (1.1) constructed above are all implicit solutions in the caes of $m \neq n$.

4.2. The case of m = n

In this scenario, Eq (2.6) becomes

$$(H^{'})^2=2\alpha_0H+\frac{4n(\omega-\sigma^2+an\kappa^2)}{a}H^2-\frac{2b}{a}H^3-\frac{4c}{3a}H^4. \tag{4.11}$$

If

$$-\frac{4c}{3a}>0,$$

i.e., $\frac{c}{a}<0$, taking the transformation

$$\Upsilon=(-\frac{4c}{3a})^{\frac{1}{4}}(H+\frac{3b}{8c}),\quad \zeta=(-\frac{4c}{3a})^{\frac{1}{4}}\xi$$

and inserting into (4.11), we yield

$$\Upsilon_\zeta^2=F(\Upsilon)=\Upsilon^4+P\Upsilon^2+G\Upsilon+R,$$

where

$$\begin{aligned}
P&=\frac{4n(\omega-\sigma^2+an\kappa^2)}{a}(-\frac{4c}{3a})^{-\frac{1}{2}},\\
G&=[2\alpha_0-\frac{9b^3+48nbc(\omega-\sigma^2+an\kappa^2)}{16ac^2}](-\frac{4c}{3a})^{-\frac{1}{4}},\\
R&=\frac{9b^2[9b^2+64nc(\omega-\sigma^2+an\kappa^2)]}{4^5ac^3}-\frac{3b\alpha_0}{4c}.
\end{aligned}$$

If

$$-\frac{4c}{3a}<0,$$

i.e., $\frac{c}{a}>0$, taking the transformation

$$\Upsilon=(\frac{4c}{3a})^{\frac{1}{4}}(H+\frac{3b}{8c}),\quad \zeta=(\frac{4c}{3a})^{\frac{1}{4}}\xi,$$

and inserting into (4.11), we yield

$$\Upsilon_\zeta^2=-F(\Upsilon)=-(\Upsilon^4+P\Upsilon^2+G\Upsilon+R),$$

where

$$P = -\frac{4n(\omega - \sigma^2 + an\kappa^2)}{a}(\frac{4c}{3a})^{-\frac{1}{2}},$$
$$G = [\frac{9b^3 + 48nbc(\omega - \sigma^2 + an\kappa^2)}{16ac^2} - 2\alpha_0](\frac{4c}{3a})^{-\frac{1}{4}},$$
$$R = \frac{3b\alpha_0}{4c} - \frac{9b^2[9b^2 + 64nc(\omega - \sigma^2 + an\kappa^2)]}{4^5ac^3}.$$

For simplicity and convenience in symbolic representation, we denote $\varepsilon = 1$, if

$$\frac{c}{a} < 0,$$

while, $\varepsilon = -1$, if

$$\frac{c}{a} > 0.$$

Then, (4.11) can be expressed as below by representing the above two situations in a combined manner:

$$\Upsilon_\zeta^2 = \varepsilon(\Upsilon^4 + P\Upsilon^2 + G\Upsilon + R). \tag{4.12}$$

Furthermore, Eq (4.12) can be rewritten as

$$\pm(\zeta - \zeta_0) = \int \frac{d\Upsilon}{\sqrt{\varepsilon(\Upsilon^4 + P\Upsilon^2 + G\Upsilon + R)}}, \tag{4.13}$$

where ζ_0 is an integral constant.

As we know, the fourth-order polynomial

$$F(\Upsilon) = \Upsilon^4 + P\Upsilon^2 + G\Upsilon + R$$

has the following complete discrimination system:

$$\begin{cases} D_1 = 4, \\ D_2 = -P, \\ D_3 = -2P^3 + 8PR - 9G^2, \\ D_4 = -P^3G^2 + 4P^4R + 36PG^2R - 32P^2R^2 - \frac{27}{4}G^4 + 64R^3, \\ E_2 = 9P^2 - 32PR. \end{cases} \tag{4.14}$$

Thus, by applying the complete discriminant method, we have the subsequent new families of traveling wave solutions for Eq (1.1):

Case 1. The rational functional solutions.

When

$$D_2 = D_3 = D_4 = 0,$$

moreover, $\varepsilon = 1$, and Eq (4.12) has the rational functional solutions

$$\Upsilon = -\frac{1}{\zeta - \zeta_0}. \tag{4.15}$$

Therefore, the solution of Eq (1.1) is

$$q_1(x,t) = [\frac{1}{\xi_0 - (-\frac{4c}{3a})^{\frac{1}{2}}(x - Vt)} - \frac{3b}{8c}]^{\frac{1}{2n}} \exp i[-\kappa x + \omega t + \sigma W(t) - \sigma^2 t]. \tag{4.16}$$

Setting parameters

$$a = -4,\ \ b = 0,\ \ c = 3,\ \ n = 2,\ \ \kappa = 1,\ \ m = 2,\ \ \sigma = 1,\ \ \xi_0 = 0,$$

the real part diagram of solution q_1 with and without random term can be intuitively shown in Figure 8. Then, changing the parameter value $m = 3, \sigma = 2$, and other parameters values remain unchanged, the real part diagram of solution q_1 with and without random term can be intuitively shown in Figure 9. As shown in the grahs, an increase in noise intensity may cause waveform distortion, typically leading to a reduction in wave stability. Additionally, variations in noise intensity may also modify the statistical properties of waves, including the distribution of wave height, trough depth, and wave period.

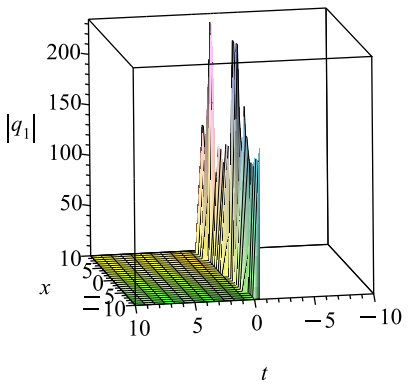

(a) 3D surface without random term

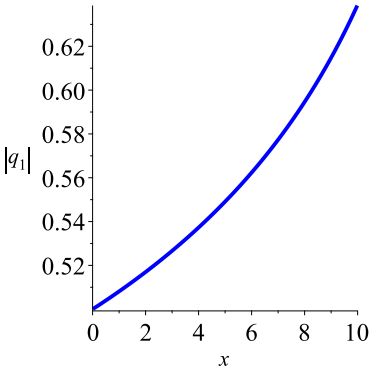

(b) 2D surface without random term

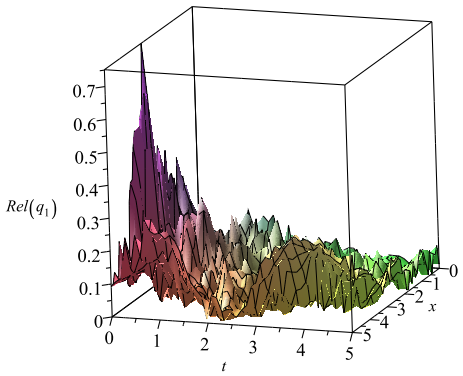

(c) 3D surface with random term

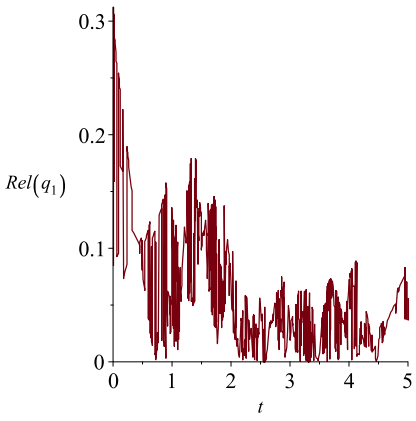

(d) 2D surface with random term

Figure 8. The solution of $Rel(q_1)$ at $a = -4, b = 0, c = 3, n = 2, \kappa = 1, m = 2, \sigma = 1$.

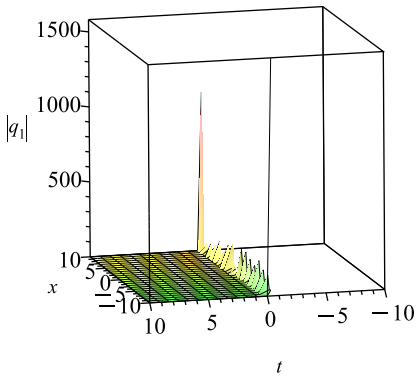

(a) 3D surface without random term

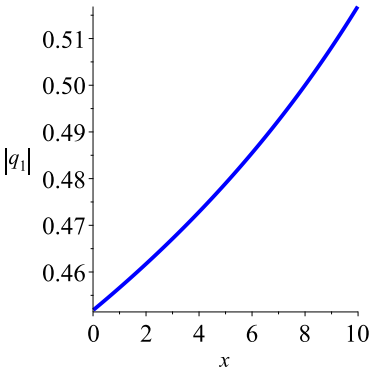

(b) 2D surface without random term

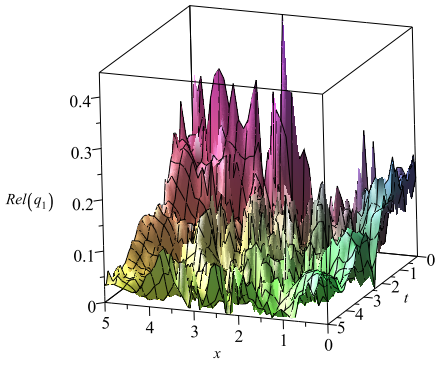

(c) 3D surface with random term

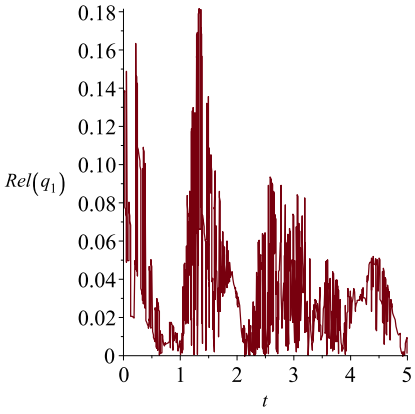

(d) 2D surface with random term

Figure 9. The solution of $Rel(q_1)$ at $a = -4, b = 0, c = 3, n = 2, \kappa = 1, m = 3, \sigma = 2$.

Case 2. The periodic solutions of triangle function.

When

$$D_2 < 0, \quad D_3 = D_4 = 0,$$

moreover, $\varepsilon = 1$, and Eq (4.12) has the periodic solution of the triangle function

$$\Upsilon = \lambda_2 \tan[\lambda_2(\zeta - \zeta_0)] + \lambda_1,$$

where λ_1 and λ_2 are two real roots of

$$F(\Upsilon) = 0$$

satisfying $\lambda_2 > 0$.

Therefore, the solution of Eq (1.1) is

$$q_2(x,t) = [(-\frac{4c}{3a})^{-\frac{1}{4}}(\lambda_2 \tan(\lambda_2(-\frac{4c}{3a})^{-\frac{1}{4}}(x - Vt) - \xi_0) + \lambda_1) - \frac{3b}{8c}]^{\frac{1}{2n}} \exp i[-\kappa x + \omega t + \sigma W(t) - \sigma^2 t]. \quad (4.17)$$

Case 3. The hyperbolic function solutions.

When

$$D_2 > 0, \quad D_3 = D_4 = 0, \quad E_2 > 0.$$

Moreover, there are two real numbers λ_3 and $\lambda_4(\lambda_3 > \lambda_4)$, which satisfy

$$F(\Upsilon) = (\Upsilon - \lambda_3)^2(\Upsilon - \lambda_4)^2 = 0.$$

And then, when $\varepsilon = 1$,

(I) If $\Upsilon > \lambda_3$ or $\Upsilon < \lambda_4$, Eq (4.12) has the solution

$$\Upsilon = \frac{\lambda_4 - \lambda_3}{2}[\coth \frac{(\lambda_3 - \lambda_4)(\zeta - \zeta_0)}{2} - 1] + \lambda_4.$$

Therefore, the solution of Eq (1.1) is

$$\begin{aligned} q_3(x,t) =&[(-\frac{4c}{3a})^{-\frac{1}{4}}(\frac{\lambda_4 - \lambda_3}{2}[\coth \frac{(\lambda_3 - \lambda_4)((-\frac{4c}{3a})^{-\frac{1}{4}}(x - Vt) - \xi_0)}{2} - 1] + \lambda_4) - \frac{3b}{8c}]^{\frac{1}{2n}} \\ &\exp i[-\kappa x + \omega t + \sigma W(t) - \sigma^2 t]. \end{aligned} \tag{4.18}$$

(II) If $\lambda_3 < \Upsilon < \lambda_4$, Eq (4.12) has the solution

$$\Upsilon = \frac{\lambda_4 - \lambda_3}{2}[\tanh \frac{(\lambda_3 - \lambda_4)(\zeta - \zeta_0)}{2} - 1] + \lambda_4.$$

Therefore, the solution of Eq (1.1) is

$$\begin{aligned} q_4(x,t) =&[(-\frac{4c}{3a})^{-\frac{1}{4}}(\frac{\lambda_4 - \lambda_3}{2}[\tanh \frac{(\lambda_3 - \lambda_4)((-\frac{4c}{3a})^{-\frac{1}{4}}(x - Vt) - \xi_0)}{2} - 1] + \lambda_4) - \frac{3b}{8c}]^{\frac{1}{2n}} \\ &\exp i[-\kappa x + \omega t + \sigma W(t) - \sigma^2 t]. \end{aligned} \tag{4.19}$$

Case 4. The implicit solutions.

When

$$D_2 > 0, \quad D_3 > 0, \quad D_4 = 0.$$

Moreover, there are three real numbers λ_5, λ_6 and $\lambda_7(\lambda_6 > \lambda_7)$, which satisfy

$$F(\Upsilon) = (\Upsilon - \lambda_5)^2(\Upsilon - \lambda_6)(\Upsilon - \lambda_7) = 0.$$

Then, when $\varepsilon = 1$, if $\lambda_5 > \lambda_6$, and $\Upsilon > \lambda_6$, or $\lambda_5 < \lambda_7$ and $\Upsilon < \lambda_7$, Eq (4.12) has the solution:

$$\pm(\zeta - \zeta_0) = \frac{1}{(\lambda_5 - \lambda_6)(\lambda_5 - \lambda_7)} \ln \frac{[\sqrt{(\Upsilon - \lambda_6)(\lambda_5 - \lambda_7)} - \sqrt{(\Upsilon - \lambda_7)(\lambda_5 - \lambda_6)}]^2}{|\Upsilon - \lambda_5|}. \tag{4.20}$$

If $\lambda_5 > \lambda_6$ and $\Upsilon < \lambda_7$, or $\lambda_5 < \lambda_7$ and $\Upsilon < \lambda_6$, Eq (4.12) has the solution:

$$\pm(\zeta - \zeta_0) = \frac{1}{(\lambda_5 - \lambda_6)(\lambda_5 - \lambda_7)} \ln \frac{[\sqrt{(\Upsilon - \lambda_6)(\lambda_7 - \lambda_5)} - \sqrt{(\Upsilon - \lambda_7)(\lambda_6 - \lambda_5)}]^2}{|\Upsilon - \lambda_5|}. \tag{4.21}$$

If $\lambda_6 > \lambda_5 > \lambda_7$, Eq (4.12) has the solution:

$$\pm(\zeta - \zeta_0) = \frac{1}{(\lambda_6 - \lambda_5)(\lambda_5 - \lambda_7)} \arcsin \frac{(\Upsilon - \lambda_6)(\lambda_5 - \lambda_7) + (\Upsilon - \lambda_7)(\lambda_5 - \lambda_6)}{|(\Upsilon - \lambda_5)(\lambda_6 - \lambda_7)|}. \tag{4.22}$$

When $\varepsilon = -1$, if $\lambda_5 > \lambda_6$ and $\Upsilon > \lambda_6$, or $\lambda_5 < \lambda_7$ and $\Upsilon < \lambda_7$, Eq (4.12) has the solution:

$$\pm(\zeta - \zeta_0) = \frac{1}{(\lambda_6 - \lambda_5)(\lambda_5 - \lambda_7)} \ln \frac{[\sqrt{(-\Upsilon + \lambda_6)(\lambda_5 - \lambda_7)} - \sqrt{(\Upsilon - \lambda_7)(\lambda_6 - \lambda_5)}]^2}{|\Upsilon - \lambda_5|}. \tag{4.23}$$

If $\lambda_5 > \lambda_6$ and $\Upsilon < \lambda_7$, or $\lambda_5 < \lambda_7$ and $\Upsilon < \lambda_6$, Eq (4.12) has the solution:

$$\pm(\zeta - \zeta_0) = \frac{1}{(\lambda_6 - \lambda_5)(\lambda_5 - \lambda_7)} \ln \frac{[\sqrt{(-\Upsilon + \lambda_6)(\lambda_7 - \lambda_5)} - \sqrt{(\Upsilon - \lambda_7)(\lambda_5 - \lambda_6)}]^2}{|\Upsilon - \lambda_5|}. \tag{4.24}$$

If $\lambda_6 > \lambda_5 > \lambda_7$, Eq (4.12) has the solution:

$$\pm(\zeta - \zeta_0) = \frac{1}{(\lambda_5 - \lambda_6)(\lambda_5 - \lambda_7)} \arcsin \frac{(-\Upsilon + \lambda_6)(\lambda_5 - \lambda_7) + (\Upsilon - \lambda_7)(\lambda_6 - \lambda_5)}{|(\Upsilon - \lambda_5)(\lambda_6 - \lambda_7)|}. \tag{4.25}$$

Case 5. The the solitary wave solutions.

When

$$D_2 D_3 < 0, \quad D_4 = 0.$$

Moreover, there are three real numbers λ_8–λ_{10}, which satisfy

$$F(\Upsilon) = (\Upsilon - \lambda_8)^2[(\Upsilon - \lambda_9)^2 + \lambda_{10}^2].$$

If $\varepsilon = 1$, Eq (4.12) has the solitary wave solution

$$\Upsilon = \frac{[e^{\pm\sqrt{(\lambda_8-\lambda_9)^2+\lambda_{10}^2}(\zeta-\zeta_0)} - \mu] + \sqrt{(\lambda_8 - \lambda_9)^2 + \lambda_{10}^2}(2 - \mu)}{[e^{\pm\sqrt{(\lambda_8-\lambda_9)^2+\lambda_{10}^2}(\zeta-\zeta_0)} - \mu]^2 - 1}, \tag{4.26}$$

where

$$\mu = \frac{\lambda_8 - 2\lambda_9}{\sqrt{(\lambda_8 - \lambda_9)^2 + \lambda_{10}^2}}.$$

Therefore, the solution of Eq (1.1) is

$$\begin{aligned} q_5(x,t) =& [(-\frac{4c}{3a})^{-\frac{1}{4}}(\frac{[e^{\pm\sqrt{(\lambda_8-\lambda_9)^2+\lambda_{10}^2}((-\frac{4c}{3a})^{-\frac{1}{4}}(x-Vt)-\xi_0)} - \mu] + \sqrt{(\lambda_8 - \lambda_9)^2 + \lambda_{10}^2}(2 - \mu)}{[e^{\pm\sqrt{(\lambda_8-\lambda_9)^2+\lambda_{10}^2}((-\frac{4c}{3a})^{-\frac{1}{4}}(x-Vt)-\xi_0)} - \mu]^2 - 1}) - \frac{3b}{8c}]^{\frac{1}{2n}} \\ & \exp i[-\kappa x + \omega t + \sigma W(t) - \sigma^2 t]. \end{aligned} \tag{4.27}$$

Setting parameters $a = -4, b = -7.032292869, c = 3, m = n = \sigma = \kappa = 1, \omega = 6, V = 8, \xi_0 = 0$, the real part diagram of solution q_5 with and without random term can be intuitively shown in Figure 10.

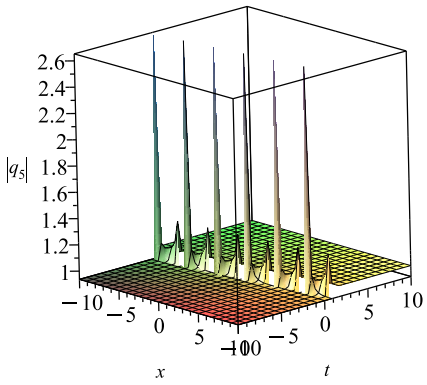

(a) 3D surface without random term

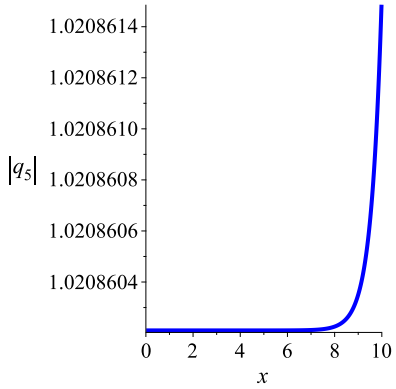

(b) 2D surface without random term

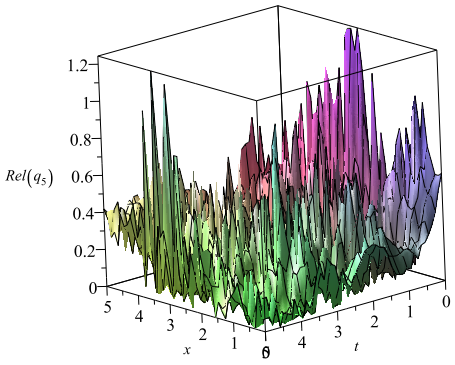

(c) 3D surface with random term

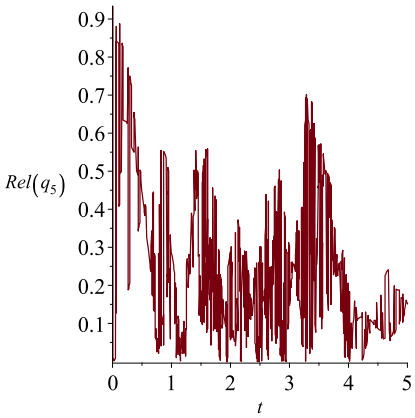

(d) 2D surface with random term

Figure 10. The solution of $Rel(q_1)$ at $a = -4, b = -7.032292869, c = 3, n = 1, \kappa = 1, m = 1, \sigma = 1$.

In the rest part, based on the definition of the Jacobian elliptic sine-cosine function, we derived the Jacobian elliptic function solutions of Eq (1.1) for three cases, designated as Cases 6–8, through trigonometric transformations.

Case 6. There are four real numbers λ_{11}, λ_{12}, λ_{13}, and $\lambda_{14}(\lambda_{11} > \lambda_{12} > \lambda_{13} > \lambda_{14})$, which satisfy

$$F(\Upsilon) = (\Upsilon - \lambda_{11})(\Upsilon - \lambda_{12})(\Upsilon - \lambda_{13})(\Upsilon - \lambda_{14}) = 0.$$

For $D_2 > 0, D_3 > 0, D_4 > 0$, when $\varepsilon = 1$, if $\Upsilon > \lambda_{11}$ or $\Upsilon < \lambda_{14}$, we consider transformation

$$\Upsilon = \frac{\lambda_{12}(\lambda_{11} - \lambda_{14})\sin^2\Psi - \lambda_{11}(\lambda_{12} - \lambda_{14})}{(\lambda_{11} - \lambda_{14})\sin^2\Psi - (\lambda_{12} - \lambda_{14})};$$

if $\lambda_{13} < \Upsilon < \lambda_{12}$, we consider transformation

$$\Upsilon = \frac{\lambda_{14}(\lambda_{12} - \lambda_{13})\sin^2\Psi - \lambda_{13}(\lambda_{12} - \lambda_{14})}{(\lambda_{12} - \lambda_{13})\sin^2\Psi - (\lambda_{12} - \lambda_{14})},$$

then we can acquire from (4.13) that

$$\begin{aligned}\zeta-\zeta_0&=\int\frac{d\Upsilon}{\sqrt{(\Upsilon-\lambda_{11})(\Upsilon-\lambda_{12})(\Upsilon-\lambda_{13})(\Upsilon-\lambda_{14})}}\\&=\frac{2}{\sqrt{(\lambda_{11}-\lambda_{13})(\lambda_{12}-\lambda_{14})}}\int\frac{d\Psi}{\sqrt{1-\Theta^2\sin^2\Psi}},\end{aligned}\tag{4.28}$$

where

$$\Theta^2=\frac{(\lambda_{11}-\lambda_{14})(\lambda_{12}-\lambda_{13})}{(\lambda_{11}-\lambda_{13})(\lambda_{12}-\lambda_{14})}.$$

Thus, the corresponding solutions of (4.12) are

$$\Upsilon=\frac{\lambda_{12}(\lambda_{11}-\lambda_{14})\mathbf{sn}^2(\frac{\sqrt{(\lambda_{11}-\lambda_{13})(\lambda_{12}-\lambda_{14})}}{2}(\zeta-\zeta_0),\Theta)-\lambda_{11}(\lambda_{12}-\lambda_{14})}{(\lambda_{11}-\lambda_{14})\mathbf{sn}^2(\frac{\sqrt{(\lambda_{11}-\lambda_{13})(\lambda_{12}-\lambda_{14})}}{2}(\zeta-\zeta_0),\Theta)-(\lambda_{12}-\lambda_{14})},\tag{4.29}$$

$$\Upsilon=\frac{\lambda_{14}(\lambda_{12}-\lambda_{13})\mathbf{sn}^2(\frac{\sqrt{(\lambda_{11}-\lambda_{13})(\lambda_{12}-\lambda_{14})}}{2}(\zeta-\zeta_0),\Theta)-\lambda_{13}(\lambda_{12}-\lambda_{14})}{(\lambda_{12}-\lambda_{13})\mathbf{sn}^2(\frac{\sqrt{(\lambda_{11}-\lambda_{13})(\lambda_{12}-\lambda_{14})}}{2}(\zeta-\zeta_0),\Theta)-(\lambda_{12}-\lambda_{14})}.\tag{4.30}$$

Here,

$$\mathbf{sn}\bigg(\frac{\sqrt{(\lambda_{11}-\lambda_{13})(\lambda_{12}-\lambda_{14})}}{2}(\zeta-\zeta_0),\Theta\bigg)=\sin\Psi.$$

Therefore, the corresponding solutions of Eq (1.1) are

$$\begin{aligned}q_6(x,t)=&\bigg((-\frac{4c}{3a})^{-\frac{1}{4}}(\frac{\lambda_{12}(\lambda_{11}-\lambda_{14})\mathbf{sn}^2(\frac{\sqrt{(\lambda_{11}-\lambda_{13})(\lambda_{12}-\lambda_{14})}}{2}((-\frac{4c}{3a})^{-\frac{1}{4}}(x-Vt)-\xi_0),\Theta)-\lambda_{11}(\lambda_{12}-\lambda_{14})}{(\lambda_{11}-\lambda_{14})\mathbf{sn}^2(\frac{\sqrt{(\lambda_{11}-\lambda_{13})(\lambda_{12}-\lambda_{14})}}{2}((-\frac{4c}{3a})^{-\frac{1}{4}}(x-Vt)-\xi_0),\Theta)-(\lambda_{12}-\lambda_{14})})\\&-\frac{3b}{8c}\bigg)^{\frac{1}{2n}}\exp i[-\kappa x+\omega t+\sigma W(t)-\sigma^2t],\end{aligned}\tag{4.31}$$

$$\begin{aligned}q_7(x,t)=&\bigg((-\frac{4c}{3a})^{-\frac{1}{4}}(\frac{\lambda_{14}(\lambda_{12}-\lambda_{13})\mathbf{sn}^2(\frac{\sqrt{(\lambda_{11}-\lambda_{13})(\lambda_{12}-\lambda_{14})}}{2}((-\frac{4c}{3a})^{-\frac{1}{4}}(x-Vt)-\xi_0),\Theta)-\lambda_{13}(\lambda_{12}-\lambda_{14})}{(\lambda_{12}-\lambda_{13})\mathbf{sn}^2(\frac{\sqrt{(\lambda_{11}-\lambda_{13})(\lambda_{12}-\lambda_{14})}}{2}((-\frac{4c}{3a})^{-\frac{1}{4}}(x-Vt)-\xi_0),\Theta)-(\lambda_{12}-\lambda_{14})})\\&-\frac{3b}{8c}\bigg)^{\frac{1}{2n}}\exp i[-\kappa x+\omega t+\sigma W(t)-\sigma^2t].\end{aligned}\tag{4.32}$$

When $\varepsilon=-1$, if $\lambda_{11}>\Upsilon>\lambda_{12}$, we consider transformation

$$\Upsilon=\frac{\lambda_{13}(\lambda_{11}-\lambda_{12})\sin^2\Psi-\lambda_{12}(\lambda_{11}-\lambda_{13})}{(\lambda_{11}-\lambda_{12})\sin^2\Psi-(\lambda_{11}-\lambda_{13})};$$

if $\lambda_{13}>\Upsilon>\lambda_{14}$, we consider transformation

$$\Upsilon=\frac{\lambda_{11}(\lambda_{13}-\lambda_{14})\sin^2\Psi-\lambda_{14}(\lambda_{13}-\lambda_{11})}{(\lambda_{13}-\lambda_{14})\sin^2\Psi-(\lambda_{13}-\lambda_{11})},$$

similarly, the corresponding solutions of (4.12) are

$$\Upsilon=\frac{\lambda_{13}(\lambda_{11}-\lambda_{12})\mathbf{sn}^2(\frac{\sqrt{(\lambda_{11}-\lambda_{13})(\lambda_{12}-\lambda_{14})}}{2}(\zeta-\zeta_0),\Theta)-\lambda_{12}(\lambda_{11}-\lambda_{13})}{(\lambda_{11}-\lambda_{12})\mathbf{sn}^2(\frac{\sqrt{(\lambda_{11}-\lambda_{13})(\lambda_{12}-\lambda_{14})}}{2}(\zeta-\zeta_0),\Theta)-(\lambda_{11}-\lambda_{13})},\tag{4.33}$$

$$\Upsilon = \frac{\lambda_{11}(\lambda_{13}-\lambda_{14})\mathbf{sn}^2(\frac{\sqrt{(\lambda_{11}-\lambda_{13})(\lambda_{12}-\lambda_{14})}}{2}(\zeta-\zeta_0),\Theta)-\lambda_{14}(\lambda_{13}-\lambda_{11})}{(\lambda_{13}-\lambda_{14})\mathbf{sn}^2(\frac{\sqrt{(\lambda_{11}-\lambda_{13})(\lambda_{12}-\lambda_{14})}}{2}(\zeta-\zeta_0),\Theta)-(\lambda_{13}-\lambda_{11})}, \tag{4.34}$$

where

$$\Theta^2 = \frac{(\lambda_{11}-\lambda_{12})(\lambda_{13}-\lambda_{14})}{(\lambda_{11}-\lambda_{13})(\lambda_{12}-\lambda_{14})}.$$

Therefore, the corresponding solutions of Eq (1.1) are

$$\begin{aligned} q_8(x,t) =& \Bigg((-\frac{4c}{3a})^{-\frac{1}{4}}\Big(\frac{\lambda_{13}(\lambda_{11}-\lambda_{12})\mathbf{sn}^2(\frac{\sqrt{(\lambda_{11}-\lambda_{13})(\lambda_{12}-\lambda_{14})}}{2}((-\frac{4c}{3a})^{-\frac{1}{4}}(x-Vt)-\xi_0),\Theta)-\lambda_{12}(\lambda_{11}-\lambda_{13})}{(\lambda_{11}-\lambda_{12})\mathbf{sn}^2(\frac{\sqrt{(\lambda_{11}-\lambda_{13})(\lambda_{12}-\lambda_{14})}}{2}((-\frac{4c}{3a})^{-\frac{1}{4}}(x-Vt)-\xi_0),\Theta)-(\lambda_{11}-\lambda_{13})}\Big) \\ &- \frac{3b}{8c}\Bigg)^{\frac{1}{2n}} \exp i[-\kappa x+\omega t+\sigma W(t)-\sigma^2 t], \end{aligned} \tag{4.35}$$

$$\begin{aligned} q_9(x,t) =& \Bigg((-\frac{4c}{3a})^{-\frac{1}{4}}\Big(\frac{\lambda_{11}(\lambda_{13}-\lambda_{14})\mathbf{sn}^2(\frac{\sqrt{(\lambda_{11}-\lambda_{13})(\lambda_{12}-\lambda_{14})}}{2}((-\frac{4c}{3a})^{-\frac{1}{4}}(x-Vt)-\xi_0),\Theta)-\lambda_{14}(\lambda_{13}-\lambda_{11})}{(\lambda_{13}-\lambda_{14})\mathbf{sn}^2(\frac{\sqrt{(\lambda_{11}-\lambda_{13})(\lambda_{12}-\lambda_{14})}}{2}((-\frac{4c}{3a})^{-\frac{1}{4}}(x-Vt)-\xi_0),\Theta)-(\lambda_{13}-\lambda_{11})}\Big) \\ &- \frac{3b}{8c}\Bigg)^{\frac{1}{2n}} \exp i[-\kappa x+\omega t+\sigma W(t)-\sigma^2 t]. \end{aligned} \tag{4.36}$$

Case 7. There are four real numbers λ_{15}–λ_{17}, and λ_{20}, which satisfy

$$F(\Upsilon) = (\Upsilon-\lambda_{15})(\Upsilon-\lambda_{16})[(\Upsilon-\lambda_{17})^2+\lambda_{18}^2]$$

and $\lambda_{15} > \lambda_{16}, \lambda_{17} > 0, \lambda_{18} > 0$. For

$$D_4 < 0, \quad D_2 D_3 \geq 0,$$

applying the transformation

$$\Upsilon = \frac{\pi_1 \cos\Psi + \pi_2}{\pi_3 \cos\Psi + \pi_4},$$

where

$$\begin{aligned} \pi_1 &= \frac{1}{2}(\lambda_{15}+\lambda_{16})\pi_3 - \frac{1}{2}(\lambda_{15}-\lambda_{16})\pi_4, \\ \pi_2 &= \frac{1}{2}(\lambda_{15}+\lambda_{16})\pi_4 - \frac{1}{2}(\lambda_{15}-\lambda_{16})\pi_3, \\ \pi_3 &= \lambda_{15}-\lambda_{17}-\frac{\lambda_{18}}{Z_3}, \quad \pi_4 = \lambda_{15}-\lambda_{17}-\lambda_{18}\Theta_1, \\ E &= \frac{\lambda_{18}^2+(\lambda_{15}-\lambda_{17})(\lambda_{16}-\lambda_{17})}{\lambda_{18}(\lambda_{15}-\lambda_{16})}, \quad \Theta_1 = E \pm \sqrt{E^2+1}, \end{aligned}$$

then we can acquire from (4.13) by this process:

$$\begin{aligned} \zeta-\zeta_0 &= \int \frac{d\Upsilon}{\sqrt{\pm(\Upsilon-\lambda_{15})(W-\lambda_{16})[(W-\lambda_{17})^2+\lambda_{18}^2]}} \\ &= \frac{2\Theta\Theta_1}{\sqrt{\mp 2\lambda_{18}\Theta_1(\lambda_{15}-\lambda_{16})}} \int \frac{d\Psi}{\sqrt{1-\Theta^2\sin^2\Psi}}, \end{aligned} \tag{4.37}$$

where

$$\Theta^2 = \frac{1}{1+\Theta_1^2}.$$

Thus, (4.12) has the elliptic double periodic function solutions as below:

$$\Upsilon = \frac{\pi_1 \mathbf{cn}\left(\frac{\sqrt{\mp 2\lambda_{18}\Theta_1(\lambda_{15}-\lambda_{16})}}{2\Theta\Theta_1}(\zeta-\zeta_0),\Theta\right)+\pi_2}{\pi_3 \mathbf{cn}\left(\frac{\sqrt{\mp 2\lambda_{18}\Theta_1(\lambda_{15}-\lambda_{16})}}{2\Theta\Theta_1}(\zeta-\zeta_0),\Theta\right)+\pi_4}. \tag{4.38}$$

Here, " $\mp$ " means that " $-$ " corresponding to $\varepsilon = 1$, and " $+$ " corresponding to $\varepsilon = -1$,

$$\mathbf{cn}\left(\frac{\sqrt{\mp 2\lambda_{18}\Theta_1(\lambda_{15}-\lambda_{16})}}{2\Theta\Theta_1}(\zeta-\zeta_0),\Theta\right) = \cos\Psi.$$

Therefore, the corresponding solutions of Eq (1.1) are

$$\begin{aligned} q_{10}(x,t) =& \left((-\frac{4c}{3a})^{-\frac{1}{4}}\left(\frac{\pi_1 \mathbf{cn}\left(\frac{\sqrt{\mp 2\lambda_{18}\Theta_1(\lambda_{15}-\lambda_{16})}}{2\Theta\Theta_1}((-\frac{4c}{3a})^{-\frac{1}{4}}(x-Vt)-\xi_0),\Theta\right)+\pi_2}{\pi_3 \mathbf{cn}\left(\frac{\sqrt{\mp 2\lambda_{18}\Theta_1(\lambda_{15}-\lambda_{16})}}{2\Theta\Theta_1}((-\frac{4c}{3a})^{-\frac{1}{4}}(x-Vt)-\xi_0),\Theta\right)+\pi_4}\right)\right. \\ &\left.-\frac{3b}{8c}\right)^{\frac{1}{2n}} \exp i[-\kappa x+\omega t+\sigma W(t)-\sigma^2 t]. \end{aligned} \tag{4.39}$$

Case 8. There are four real numbers λ_{19}–λ_{22}, which satisfy

$$F(\Upsilon) = [(\Upsilon-\lambda_{19})^2+\lambda_{20}^2][(\Upsilon-\lambda_{21})^2+\lambda_{22}^2]$$

and $\lambda_{20} \geq \lambda_{22} > 0$. Then, for $D_4 > 0, D_2D_3 \leq 0$,

When $\varepsilon = 1$, applying the transformation

$$\Upsilon = \frac{\pi_5 \tan\Psi + \pi_6}{\pi_7 \tan\Psi + \pi_8},$$

where

$$\begin{aligned} &\pi_5 = \lambda_{19}\pi_7 + \lambda_{20}\pi_8,\ \ \pi_6 = \lambda_{19}\pi_8 - \lambda_{20}\pi_7,\ \ \pi_7 = -\lambda_{20} - \frac{\lambda_{22}}{\Theta_1},\ \ \pi_8 = \lambda_{19}-\lambda_{21}, \\ &E = \frac{(\lambda_{19}-\lambda_{21})^2+\lambda_{20}^2+\lambda_{22}^2}{2\lambda_{20}\lambda_{22}},\ \ \Theta_1 = E+\sqrt{E^2-1}, \end{aligned}$$

we can acquire from (4.13) that

$$\zeta-\zeta_0 == \frac{\pi_7^2+\pi_8^2}{\lambda_{22}\sqrt{(\pi_7^2+\pi_8^2)(\Theta_1^2\pi_7^2+\pi_8^2)}}\int \frac{d\Psi}{\sqrt{1-\Theta^2\sin^2\Psi}}, \tag{4.40}$$

where

$$\Theta^2 = \frac{\Theta_1^2-1}{\Theta_1^2}.$$

Thus, Eq (4.12) has the elliptic double periodic function solutions as below:

$$\Upsilon = \frac{\pi_5 \mathbf{sn}\Big(\Xi(\zeta-\zeta_0),\Theta\Big) + \pi_6 \mathbf{cn}\Big(\Xi(\zeta-\zeta_0),\Theta\Big)}{\pi_7 \mathbf{sn}\Big(\Xi(\zeta-\zeta_0),\Theta\Big) + \pi_8 \mathbf{cn}\Big(\Xi(\zeta-\zeta_0),\Theta\Big)}, \tag{4.41}$$

where

$$\Xi = \frac{\lambda_{22}\sqrt{(\pi_7^2+\pi_8^2)(\Theta_1^2\pi_7^2+\pi_8^2)}}{\pi_7^2+\pi_8^2},$$
$$\mathbf{sn}\Big(\frac{\lambda_{22}\sqrt{(\pi_7^2+\pi_8^2)(\Theta_1^2\pi_7^2+\pi_8^2)}}{\pi_7^2+\pi_8^2}(\zeta-\zeta_0),\Theta\Big) = \sin\Psi,$$
$$\mathbf{cn}\Big(\frac{\lambda_{22}\sqrt{(\pi_7^2+\pi_8^2)(\Theta_1^2\pi_7^2+\pi_8^2)}}{\pi_7^2+\pi_8^2}(\zeta-\zeta_0),\Theta\Big) = \cos\Psi.$$

Therefore, the solution of Eq (1.1) is

$$\begin{aligned} q_{11}(x,t) =& \Big((-\frac{4c}{3a})^{-\frac{1}{4}}\Big(\frac{\pi_5 \mathbf{sn}\Big(\Xi((-\frac{4c}{3a})^{-\frac{1}{4}}(x-Vt)-\xi_0),\Theta\Big) + \pi_6 \mathbf{cn}\Big(\Xi((-\frac{4c}{3a})^{-\frac{1}{4}}(x-Vt)-\xi_0),\Theta\Big)}{\pi_7 \mathbf{sn}\Big(\Xi((-\frac{4c}{3a})^{-\frac{1}{4}}(x-Vt)-\xi_0),\Theta\Big) + \pi_8 \mathbf{cn}\Big(\Xi((-\frac{4c}{3a})^{-\frac{1}{4}}(x-Vt)-\xi_0),\Theta\Big)}\Big) \\ & - \frac{3b}{8c}\Big)^{\frac{1}{2n}} \exp i[-\kappa x + \omega t + \sigma W(t) - \sigma^2 t]. \end{aligned} \tag{4.42}$$

5. Conclusions

In this study, we consider the dynamical behavior and new traveling wave solution of the stochastic BME with dual-power law nonlinearity and multiplicative white noise in the Itô sense. The qualitative analysis of the dynamical system of Eq (1.1) and its perturbation system are considered though the principle of homogeneous balance and the planar dynamical system method. Then, we draw 2D phase portraits of the dynamical system and easily observe the orbital properties of the dynamical system. Considering that periodic interference often exists in real environments, we add the periodic disturbance term to system (3.2), and then the 2D and 3D phase portrait, sensitivity analyses, and Poincaré section of its perturbation system are plotted by the Maple software. Moreover, by using the complete discrimination system method, the new traveling wave solutions of Eq (1.1) are successfully constructed with the effect of the Wiener process implicated. Compared with existing literature, the research findings of this article contribute to make a comprehensive and systemic study on the propagation dynamics of the stochastic BME with dual-power law nonlinearity and multiplicative white noise in the Itó sense Eq (1.1) with different methods. Specifically, we have not only enriched the solutions of the BME but also conducted a thorough analysis of the planar dynamical system. The findings we have obtained provide insight into the chaotic nature of the framework under examination, thereby enhancing our understanding of the dynamics that underlie it. The research methods employed in this work are highly reliable, versatile, and effective for a variety of nonlinear models across different scientific disciplines.

Author contributions

Dan Chen: writing–original draft, writing–review & editing; Da Shi: supervision; Feng Chen: software. All authors have read and agreed to the published version of the manuscript.

Use of Generative-AI tools declaration

The authors declare they have not used Artificial Intelligence (AI) tools in the creation of this article.

Acknowledgments

This project is supported by funding of Visual Computing and Virtual Reality Key Laboratory of Sichuan Province via grant (No. SCVCVR2023.06VS).

Conflict of interest

The authors declare no conflicts of interest.

References

1. M. Ozisik, A. Secer, M. Bayram, Discovering optical soliton solutions in the Biswas-Milovic equation through five innovative approaches, *Optik*, **286** (2023), 170986. https://doi.org/10.1016/j.ijleo.2023.170986
2. N. M. Elsonbaty, N. M. Badra, H. M. Ahmed, A. M. Elsherbeny, Derivation of new optical solitons for Biswas-Milovic equation with dual-power law nonlinearity using improved modified extended tanh-function method, *Alex. Eng. J.*, **67** (2023), 537–546. https://doi.org/10.1016/j.aej.2022.12.068
3. E. M. E. Zayed, A. G. Al-Nowehy, Exact solutions and optical soliton solutions of the nonlinear Biswas-Milovic equation with dual-power law nonlinearity, *Acta Phys. Pol. A.*, **131** (2017), 240–251. https://doi.org/10.12693/APhysPolA.131.240
4. A. Khan, S. Saifullah, S. Ahmad, M. A. Khan, M. Rahman, Dynamical properties and new optical soliton solutions of a generalized nonlinear Schrödinger equation, *Eur. Phys. J. Plus*, **138** (2023), 1059. https://doi.org/10.1140/epjp/s13360-023-04697-5
5. A. Ali, J. Ahmad, S. Javed, Exploring the dynamic nature of soliton solutions to the fractional coupled nonlinear Schrödinger model with their sensitivity analysis, *Opt. Quant. Electron.*, **55** (2023), 810. https://doi.org/10.1007/s11082-023-05033-y
6. D. Chen, Z. Li, Optical solitons and single traveling wave solutions for the fiber Bragg gratings with generalized anticubic nonlinearity, *Adv. Math. Phys.*, 2023. https://doi.org/10.1155/2023/6283436
7. C. M. Khalique, Stationary solutions for the Biswas-Milovic equation, *Appl. Math. Comput.*, **217** (2011), 7400–7404. https://doi.org/10.1016/j.amc.2011.02.028
8. A. Prakash, H. Kaur, Analysis and numerical simulation of fractional Biswas-Milovic model, *Math. Comput. Simul.*, **181** (2021), 298–315. https://doi.org/10.1016/j.matcom.2020.09.016

9. N. A. Shah, H. A. Alyousef, S. A. El-Tantawy, R. Shah, J. D. Chung, Analytical investigation of fractional-order Korteweg-de-Vries-Type equations under Atangana-Baleanu-Caputo operator: modeling nonlinear waves in a plasma and fluid, *Symmetry*, **14** (2022), 739. https://doi.org/10.3390/sym14040739

10. A. Moumen, K. A. Aldwoah, M. Suhail, A. Kamel, H. Saber, M. Hleili, et al., Investigation of more solitary waves solutions of the stochastics Benjamin-Bona-Mahony equation under beta operator, *AIMS Math.*, **9** (2024), 27403–27417. https://doi.org/10.3934/math.20241331

11. J. Ahmad, S. Akram, S. U. Rehman, N. B. Turki, N. A. Shah, Description of soliton and lump solutions to M-truncated stochastic Biswas-Arshed model in optical communication, *Results Phys.*, **51** (2023), 106719. https://doi.org/10.1016/j.rinp.2023.106719

12. L. F. Guo, W. R. Xu, The traveling wave mode for nonlinear Biswas-Milovic equation in magneto-optical wave guide coupling system with Kudryashov's law of refractive index, *Results Phys.*, **27** (2021), 104500. https://doi.org/10.1016/j.rinp.2021.104500

13. M. Shakeel, Attaullah, N. A. Shah, J. D. Chung, Application of modified exp-function method for strain wave equation for finding analytical solutions, *Ain Shams Eng. J.*, **14** (2023), 101883. https://doi.org/10.1016/j.asej.2022.101883

14. A. H. Arnous, M. S. Hashemi, K. S. Nisar, M. Shakeel, J. Ahmad, I. Ahmad, et al., Investigating solitary wave solutions with enhanced algebraic method for new extended Sakovich equations in fluid dynamics, *Results Phys.*, **57** (2024), 107369. https://doi.org/10.1016/j.rinp.2024.107369

15. N. A. Shah, E. R. El-Zahar, A. Akgül, A. Khan, J. Kafle, Analysis of fractional-order regularized long-wave models via a novel transform, *J. Funct. Spaces*, **2022** (2022), 2754057. https://doi.org/10.1155/2022/2754507

16. X. X. Zheng, Y. Shang, Abundant explicit exact solutions to the generalized nonlinear Schrödinger equation with parabolic law and dual power law nonlinearities, *Math. Methods Appl. Sci.*, **38** (2015), 296–310. https://doi.org/10.1002/mma.3069

17. Douvagai, Y. Salathiel, G. Betchewe, S. Y. Doka, K. T. Crepin, Exact traveling wave solutions to the fourthorder dispersive nonlinear Schrödinger equation with dual-power law nonlinearity, *Math. Methods Appl. Sci.*, **39** (2016), 1135–1143. https://doi.org/10.1002/mma.3557

18. F. Tchier, E. C. Aslan, M. Inc, Optical solitons in parabolic law medium: Jacobi elliptic function solution, *Nonlinear Dyn.*, **85** (2016), 2577–2582. https://doi.org/10.1007/s11071-016-2846-6

19. W. J. Zhu, J. B. Li, Exact traveling wave solutions and bifurcations of the Biswas-Milovic equation, *Nonlinear Dyn.*, **84** (2016), 1973–1987. https://doi.org/10.1007/s11071-016-2621-8

20. A. Ali, J. Ahmad, S. Javed, S. U. Rehman, Analysis of chaotic structures, bifurcation and soliton solutions to fractional Boussinesq model, *Phys. Scr.*, **98** (2023), 075217. https://doi.org/10.1088/1402-4896/acdcee

21. J. B. Li, Y. Zhou, Bifurcations and exact traveling wave solutions for the nonlinear Schrödinger equation with fourth-order dispersion and dual power law nonlinearity, *Discrete Cont. Dyn. Syst.*, **13** (2020), 3083–3097. https://doi.org/10.3934/dcdss.2020113

22. E. M. E. Zayed, R. M. A. Shohib, M. E. M. Alngar, Dispersive optical solitons with Biswas-Milovic equation having dual-power law nonlinearity and multiplicative white noise via Itó calculus, *Optik*, **270** (2022), 169951. https://doi.org/10.1016/j.ijleo.2022.169951

23. C. S. Liu, A new trial equation method and its applications, *Commun. Theor. Phys.*, **45** (2006), 296–310. https://doi.org/10.1088/0253-6102/45/3/003

24. Z. Li, S. Zhao, Bifurcation, chaotic behavior and solitary wave solutions for the Akbota equation, *AIMS Math.*, **9** (2024), 22590–22601. https://doi.org/10.3934/math.20241100

25. Z. Li, J. J. Lyu, E. Hussain, Bifurcation, chaotic behaviors and solitary wave solutions for the fractional Twin-Core couplers with Kerr law non-linearity, *Sci. Rep.*, **14** (2024), 22616. https://doi.org/10.1038/s41598-024-74044-w

AIMS Press